ELSEVIER

Polymer 44 (2003) 2143–2148

polymer

www.elsevier.com/locate/polymer

Synthesis and optically acid-sensory properties of novel polyoxadiazole derivatives

Nam Choul Yang[a], Seok Chang[b], Dong Hack Suh[a,*]

[a]School of Chemical Engineering, College of Engineering, Hanyang University, 17 Haengdang 1-dong, Seongdong-gu, Seoul 133-791, South Korea
[b]Samsung Advanced Institute of Technology, P.O. Box 111, Suwon 400-600, South Korea

Received 2 August 2002; received in revised form 7 December 2002; accepted 20 December 2002

Abstract

New organo-soluble and blue-emissive fluorene-based polyoxadiazoles, PFO$_x$ and PFO$_x$EH, exhibit colorimetric and fluorescent acid-sensory properties to a strong acid due to the weak basicity of imine-type nitrogen atom(s) in an 1,3,4-oxadiazole ring. To further investigate their protonation with an acid, ^{1}H NMR spectroscopy and AM1 semiempirical quantum-mechanics are utilized as well as UV–visible absorption and fluorescence spectroscopies. These investigations indicate the protonation does not proceed thermodynamically but kinetically at the initial stage of the complex formation of an acid and an oxadiazole ring in the polymer backbone.

Keywords: Polyoxadiazole; Conjugated polymer sensor; Fluorescence

1. Introduction

Chemical sensors based on conjugated polymers recently have attracted considerable interests due to their some merits over the sensor systems based on small molecules such as the enhanced sensitivity, many transduction methods, high thermal stability, facile processibility for condensed phase applications and robust mechanical strength [1,2]. The semiconductive molecular structure formed along the conjugated polymer chain provides transductional amplification and various transduction signals such as optical absorption, fluorescence and electrical conductivity [2]. Many conjugated polymers having imine-type (C=N) nitrogen atom(s) in a heterocycle unit, such as pyridine [3,4], quinoline [5,6], benzoazole [7,8] and benzeimidazole [9,10], have been reported to exhibit colorimetric and fluorescent acid-sensory properties. Revelation and the extent of acid-sensory transduction depend on both basicity of heterocycles and the structure of the conjugated polymer including the effective conjugation length and CT characteristics [2]. So acid-sensory properties can be regulated by tuning the chemical structure of a conjugated polymer.

On the other hand, it has been reported that the solvent system using a Lewis acid such as $AlCl_3$, $FeCl_3$ and $GaCl_3$ is useful for solubilizing polyoxadiazoles [11]. This solution preparation method was described for the first time for aromatic heterocyclic rigid rod polymers such as polybenzoxazoles, polybenzothiazoles and polybenzimidazoles [7,9,12]. Through the quantitative analysis of the effect of this solvent system on polyoxadiazoles, it was found that the interaction between the imine-type nitrogen atoms of an oxadiazole ring and a Lewis acid is the key point of the enhancement of the polymer solubility [13]. However, to our knowledge, there has been no report about the influence of the complex formation with an acid to optical properties of aromatic polyoxadiazoles.

Recently, we reported synthesis and characterization of a series of fluorene-based polyoxadiazoles with efficient blue fluorescence properties as electroluminescent or chemical sensor materials [14]. In that report, we briefly described the solubility enhancement and optical changes by adding trifluoroacetic acid to the polymer solution. In this article, we describe the further investigation of optical changes of new fluorene-based polyoxadiazole derivatives, PFO$_x$ and PFO$_x$EH, caused by the complex formation with an acid.

---

* Corresponding author. Tel.: +82-2-2290-0523; fax: +82-2-2282-0523.
E-mail address: dhsuh@hanyang.ac.kr (D.H. Suh).

0032-3861/03/$ - see front matter © 2003 Elsevier Science Ltd. All rights reserved.
PII: S0032-3861(02)00936-9

2. Experimental

2.1. Materials

All chemical reagents were purchased from Aldrich, Acros and TCI and used without further purification. 9,9-Didodecylfluorene-2,7-dicarboxylic acid was synthesized according to the previously reported procedure [14].

2.2. Synthesis

2.2.1. Poly[(9,9-didodecylfluorene-2,7-diyl)-alt-(1,3,4-oxadiazole-2,5-diyl)] (PFO$_x$)

In a 25 mL three-necked flask under a dry nitrogen flux, 9,9-didodecylfluorene-2,7-dicarboxylic acid (0.296 g, 0.5 mmol) and hydrazine sulfate (0.065 g, 0.5 mmol) were added to PPMA (10% P_2O_5 in CH_3SO_3H) (5 mL). While stirring, the solution was heated to 80 °C for 1 h and then 120 °C for 2 h under N_2. The viscous gum clung to a stirrer. The resultant gum was poured into a diluted NaOH solution, crushed with a spatula, filtered off, washed with water and methanol several times and dried at 80 °C in vacuo. After twice precipitation from the polymer solution in a mixture of 1,2-dichloroethane/trifluoroacetic acid (10:1 mL) into methanol/triethylamine (350:50 mL), the fibrous gray powder of PFO$_x$ was obtained with the yield of 0.20 g (98%). Analytical data of PFO$_x$: ^{1}H NMR ($CDCl_3$, ppm): $\delta = 8.25$ (s(br), 4H), 8.00 (s(br), 2H), 2.20 (br, 4H), 1.18 (br, 36H), 0.83 (br, 4H), 0.69 (br, 6H); ^{13}C NMR ($CDCl_3$, ppm): $\delta = 165.1$, 152.4, 143.5, 126.4, 123.5, 121.6, 121.1, 56.0, 40.3, 31.8, 29.5 (br), 23.9, 22.6, 14.0; IR (KBr, cm^{-1}): 3080 and 3045 (aromatic C–H), 2925 and 2853 (aliphatic C–H), 1613, 1591, 1541 (C=N in oxadiazole), 1461, 1413, 1377, 1249, 1065, 966 (C–O–C in oxadiazole), 893, 828, 739.

2.2.2. Poly{(9,9-didodecylfluorene-2,7-diyl)-alt-[(1,4-bis(1,3,4-oxadiazole)-2,5-di(2-ethylhexyloxy)-phenylene)-5,5′-diyl]} (PFO$_x$EH) [14]

9,9-Didodecylfluorene-2,7-dicarboxylic acid (0.591 g, 1.0 mmol), 2,5-di(2-ethylhexyloxy)terephthalic dihydrazide (0.450 g, 1.0 mmol), LiCl (0.2 g) and triphenylphosphite (0.683 g, 2.2 mmol) were dissolved in a mixture of *N*-methylpyrrolidinone (4 mL) and pyridine (1 mL). The solution was stirred at 105 °C for 5 h under N_2 and then poured into methanol. After filtered, washed with methanol and water several times and dried at 80 °C in vacuo, the white fibrous precipitate of a polyhydrazide (PrePFO$_x$EH) was obtained with the yield of 0.995 g (99%) as a polyoxadiazole precursor. Then, PrePFO$_x$EH (0.772 g) in $POCl_3$ (25 mL) was refluxed for 5 h under N_2 and then poured into water. After filtered, washed with a mixture of methanol and triethylamine and water several times and dried at 80 °C in vacuo, the pale yellow fibrous precipitate of PFO$_x$EH was obtained with the yield of 0.737 g (99%). Analytical data of PFO$_x$EH: ^{1}H NMR ($CDCl_3$, ppm): $\delta = 8.23$ (s(br), 4H), 8.15 (s(br), 4H), 4.16 (br, 4H), 0.62–2.18 (m (br), 80H); ^{13}C NMR ($CDCl_3$, ppm): $\delta = 165.9$, 163.5, 152.3, 151.0, 143.5, 126.4, 123.5, 121.4, 121.0, 116.6, 114.6, 71.5, 56.1, 40.4, 39.7, 31.9, 30.7, 29.6 (br), 24.0, 23.1, 22.7, 14.1, 11.1; IR (KBr, cm^{-1}): 3045, 2956, 2925 and 2854, 1551 (C=N in oxadiazole), 1461, 1219, 1071, 1033 (C–O–C in oxadiazole), 828, 748.

2.3. Instrumental

^{1}H and ^{13}C NMR spectra were obtained using a Varian VXR-300 FT-NMR spectroscopy (300 MHz) relative to tetramethylsilane as an internal standard. IR spectra were recorded on a Nicolet 360 FT-IR spectrometer. To determine molecular weights of a polymer, gel permeation chromatography (GPC) was carried out using a Waters GPC system equipped with a differential refractometer and Ultrastyragel columns in series at room temperature. Thermogravimetric analysis (TGA) and differential scanning calorimetry (DSC) were conducted with TA instruments SDT 2960 Simultaneous DSC-TGA and DSC 2010 units, respectively, under a nitrogen atmosphere. UV–visible absorption and fluorescence spectra were recorded on a Shimadzu UV-2101PC UV–VIS scanning spectrophotometer and a Shimadzu RF 5301PC Spectrofluorophotometer, respectively. The fluorescence quantum yield was determined in comparison with that of 9,10-diphenylanthracene in cyclohexane according to the well-known method [15].

2.4. Computations

AM1 semiempirical quantum-mechanical calculations were carried out with the Hypercube Hyperchem v. 6.03 to estimate optimized geometry and frontier orbital energies of molecules. AM1 self-consistent field calculation was carried out under the condition of convergence limit of 0.01 kcal/mol and spin interactions of the restricted Hartree-Fock method.

3. Results and discussion

Various methods have been carried out in order to prepare poly(1,3,4-oxadiazole)s. In large, the preparation method of polyoxadiazoles can be classified by the one-step and the two-step method via polyhydrazide precursors [11, 16]. PFO$_x$ was prepared by the conventional one-step method using PPMA as both a polymerization solvent and a dehydration reagent which has been known as a simple method for high molecular weight polyoxadiazoles [17]. However, the preparation of PFO$_x$EH using the same one-step method was unsuccessful due to the decomposition of 2,5-di(2-ethylhexyloxy)terephthalic dihydrazide in acidic PPMA under a high temperature condition. So we used the two-step method for PFO$_x$EH which has some advantages over the one-step method such as the usage of acid-sensitive monomers and the relatively low preparation temperature. A polyhydrazide, PrePFO$_x$EH, of the precursor of PFO$_x$EH was prepared by a phosphorylation polyamidation known as a Yamazak-Higashi reaction [17]. Then, PrePFO$_x$EH was converted to PFO$_x$EH using $POCl_3$ at a reflux condition [18, 19]. The chemical structures of PFO$_x$ and PFO$_x$EH were confirmed by IR and NMR spectroscopies, which indicates that their synthesis was successfully carried out. (Scheme 1)

The polymers show relatively high molecular weight, determined by GPC with tetrahydrofuran (THF) as an eluent (Table 1). PFO$_x$ and PFO$_x$EH are soluble in some common organic solvents such as THF, 1,2-dichloroethane (DCE), trichloroethylene and chlorobenzene. However, at high concentration (>10 mg/mL), the polymers are partially soluble at room temperature showing a little turbidity. On adding a little amount of trifluoroacetic acid (TFAA) to the polymer solution, the polymers are clearly soluble, which indicates the interaction between the oxadiazole unit in their main chain and TFAA including the acid–base reaction [18, 19].

Thermal properties of the polymers were analyzed by TGA and DSC, of which the results are listed in Table 1. TGA results of the polymers reveal that they are stable up to ca. 350 °C under a nitrogen atmosphere. Estimated by DSC, the grass transition temperatures (T_g) of PFO$_x$ and PFO$_x$EH are 119 and 99 °C, respectively.

PFO$_x$ and PFO$_x$EH show blue fluorescence with the maximum bands at 399 and 421 nm, respectively (Figs. 1 and 2), and significantly high fluorescence quantum yields of 1.00 and 0.84, respectively. The UV–visible absorption and fluorescence spectra of PFO$_x$EH show red-shift relative to those of PFO$_x$ by ca. 20 nm, which indicates that the electron-donating effect of a dialkoxyphenylene unit in PFO$_x$EH decreases its band gap relative to PFO$_x$.

Table 1
Molecular weights and thermal properties of PFO$_x$ and PFO$_x$EH

Polymer	$M_w \times 10^{-3a}$	$M_n \times 10^{-3b}$	PDI[c]	T_d (°C)[d]	T_g (°C)[e]
PFO$_x$	80.1	37.6	2.13	423	119
PFO$_x$EH	120.5	36.3	3.32	358	99

[a] The weight-average molecular weight determined by GPC.

[b] The number-average molecular weight determined by GPC.

[c] Polydispersity index, PDI = M_w/M_n.

[d] Glass transition temperature measured by DSC (N_2, 5 °C/min).

[e] Decomposition onset temperature measured by TGA (N_2, 10 °C/min).

An 1,3,4-oxadiazole ring can be thought to be a basic heterocycle due to the presence of imine-type nitrogen atoms with its lone pair electrons not participating in the aromatic sextet. Trifonov et al. reported that 2,5-diphenyl-1,3,4-oxadiazole displays a very weak basic property (p$K_{BH}+$, -1.83) determined by fluorescence spectroscopy [20]. Oxadiazole-based PFO$_x$ and PFO$_x$EH also exhibit fluorescence quenching by the addition of a strong acid such as hydrogen chloride (pK_a, -6.1), sulfuric acid (pK_a, -2.8), methanesulfonic acid (pK_a, -1.9) and TFAA (pK_a, 0.5). However, they do not respond to relatively weak acids (approximately positive pK_a) such as phosphoric acid, formic acid and acetic acid due to the very weak basicity of an oxadiazole ring in their main chains.

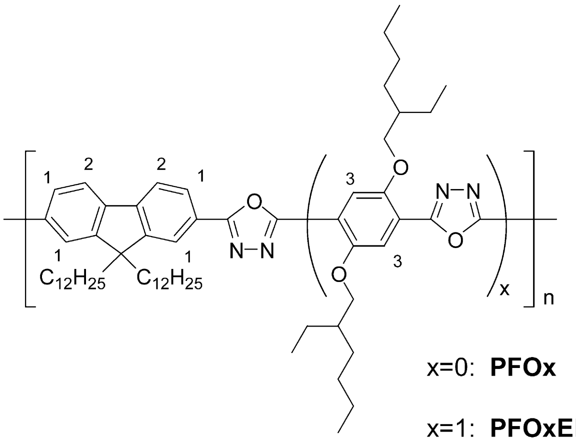

Scheme 1. The chemical structures of PFO$_x$ and PFO$_x$EH. The assignments indicate aromatic protons for their ^{1}H NMR spectra.

As shown in Figs. 1(a) and 2(a), the UV–visible spectra

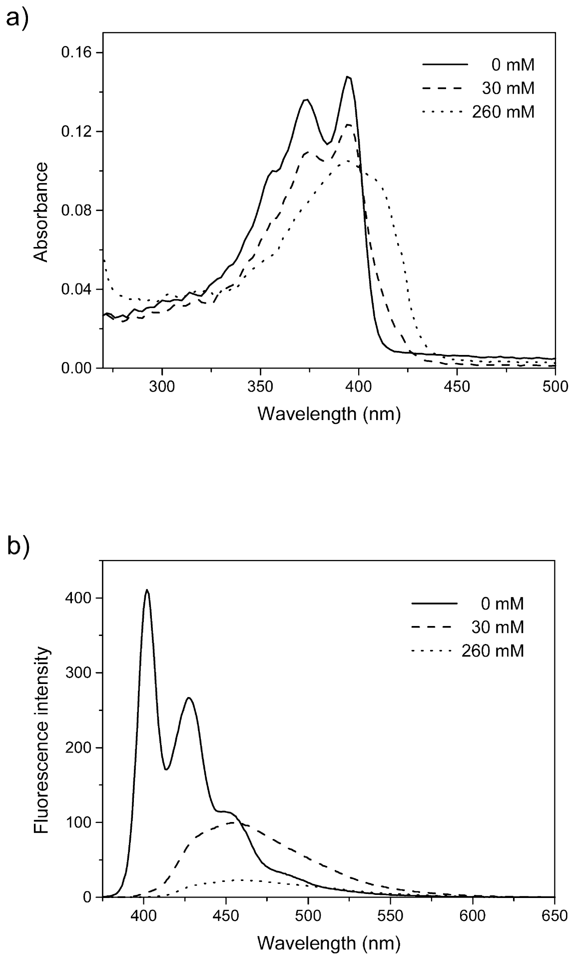

Fig. 1. UV–visible absorption (a) and fluorescence (b) spectrum changes of PFO$_x$ in DCE (1×10^{-6} M) upon the addition of TFAA.

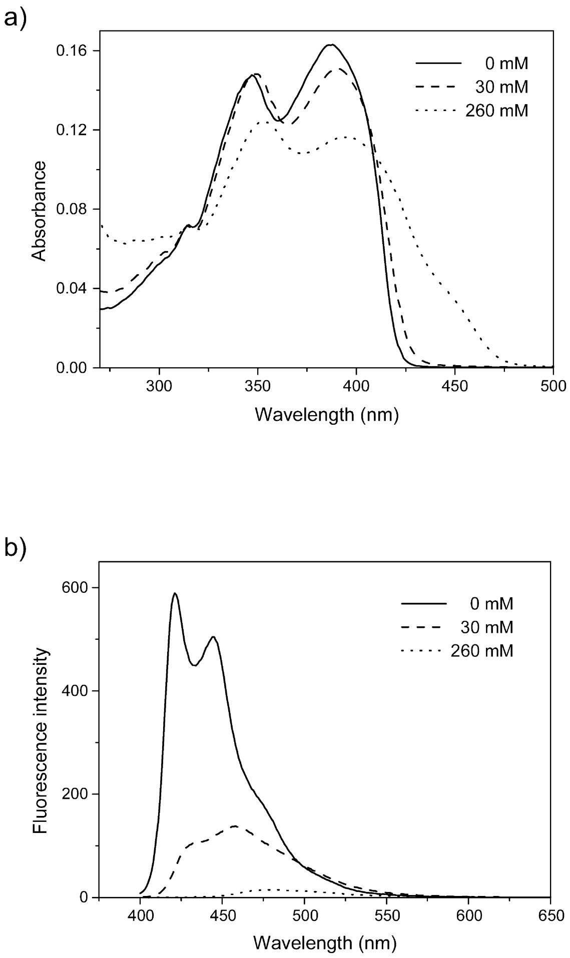

Fig. 2. UV–visible absorption (a) and fluorescence (b) spectrum changes of PFO_xEH in DCE (1×10^{-6} M) upon the addition of TFAA.

of PFO_x and PFO_xEH solution are changed with the amount of added TFAA. Increasing the amount of TFAA, the absorption maximum band is both bathochromically and hypochromically shifted due to protonation-induced enhancement of intramolecular charge transfer (CT) which is well-known phenomena for aromatic heterocyclic polymers [3,5,6,21,22].

Figs. 1(b) and 2(b) show the acid-concentration dependence of the fluorescence of the polymers. Compared with UV–visible absorption spectra, the transductive effect of protonation on the fluorescence spectra is large. Increasing the amount of TFAA, the fluorescence of both polymers becomes significantly quenched. As protonation-induced quenching is saturated, PFO_x and PFO_xEH show the quenched and red-shifted fluorescence spectrum with maximum bands at 461 and 471 nm, respectively. The effective fluorescence transduction property of the polymers may be due to following reasons: the inherent high sensitivity of fluorescence transductional signals [2], the increased proton affinity of an oxadiazole ring in the excited state in comparison with that in the ground state [23] and the amplified transduction effect of fluorescence quenching by the proton or energy transfer through the conjugated chain structure [1,2]. Both the quenching and the red-shift of fluorescence, caused by the protonation, can be explained by the electron or energy transfer from a non-protonated to a protonated part with the lower-lying and more narrowed electronic energy band gap than non-protonated one via an intramolecular and/or intermolecular pathway(s) [24].

Figs. 3 and 4 display the protonation effect on ^{1}H NMR spectra of PFO_x and PFO_xEH. As shown in Fig. 3, PFO_x dissolved in $CDCl_3$ shows aromatic proton peaks in a fluorene unit at $\delta = 8.26$ ppm (1-position) and 8.00 ppm (2-position). However, in its NMR spectrum dissolved in a mixture of $CDCl_3$ and CF_3CO_2D (TFAA-*d*), one aromatic proton peak at 2-position in the pristine state shifts to $\delta = 8.10$ ppm, which shows that the protonation at a nitrogen atom of imine in an oxadiazole group. The π-deficiency of an oxadiazole group is enhanced by the protonation, which causes the down-field shift of protons in the adjacent fluorene group. On the other hand, as shown in Fig. 4, signals of aromatic protons in a fluorene unit (2-position) and a phenylene unit (3-position) are overlapped at $\delta = 8.15$ ppm in the pristine state of PFO_xEH, so its aromatic protons seem to show the simple pattern of two peaks at $\delta = 8.23$ and 8.15 ppm. However, as TFAA-*d* is introduced to this $CDCl_3$ solution of PFO_xEH, signals of protons at $\delta = 8.15$ ppm splits; the signals of the protons in the fluorene unit (2-position) shift to the down-field region relative to those in the pristine sample, whereas those in the phenylene unit (3-position) shift to the up-field region. In addition, the degree of the shift of the proton signals of 1-position in the fluorene unit is relatively very small in comparison with other aromatic proton signals. This reason is the charge separation induced by the protonation of a nitrogen atom in an oxadiazole ring. Polyoxadiazoles can be thought to have the structure exhibiting intramolecular CT

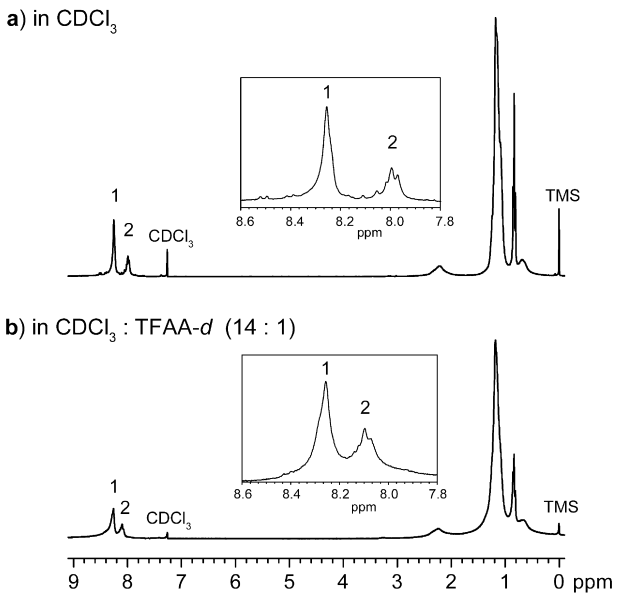

Fig. 3. ^{1}H NMR spectra of PFO_x in (a) $CDCl_3$ and (b) $CDCl_3$/TFAA-*d* (14:1). Inserted graphs show proton signals of aromatic regions.

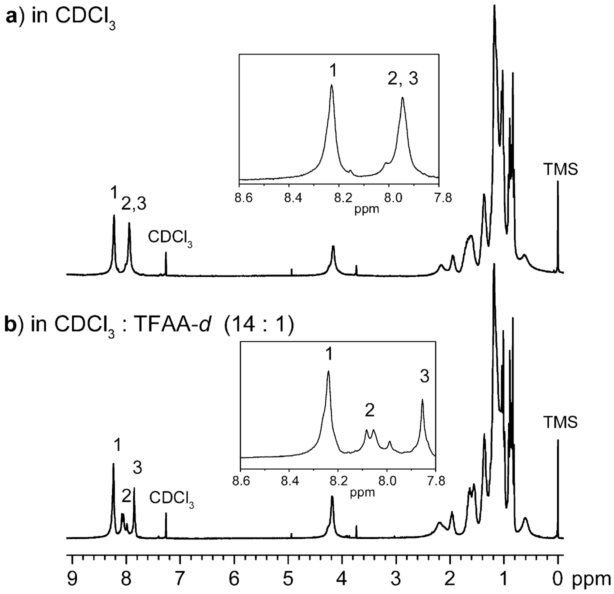

Fig. 4. ^{1}H NMR spectra of PFO$_x$EH in (a) CDCl$_3$ and (b) CDCl$_3$/TFAA-*d* (14:1). Inserted graphs show proton signals of aromatic regions.

between the electron-deficient oxadiazole and other relatively electron-excessive aromatic group. Electron-donating alkoxy groups at the phenylene group in the main chain of PFO$_x$EH should enhance the intramolecular CT. The protonation of a nitrogen atom in an oxadiazole unit still more increases the intramolecular CT of the molecule and, as a result, the charge separation is maximized. Protons (2-position) in a fluorene group having less electron-donability than dialkoxy phenylene are shifted to the down-field region, whereas those in a phenylene group (3-position) are shifted to the up-field region due to the relatively increased electron density localization by the charge separation.

We carry out the computational calculation of the model compound of PFO$_x$EH, 2-[5-(*p*-dimethoxyphenyl)-1,3,4-oxadiazole]-9,9-dimethylfluorene (FO$_x$P), to obtain the more precise description of the above NMR result [25]. The geometry optimization of FO$_x$P and the determination of the distribution of the frontier molecular orbitals (MO) in FO$_x$P are performed using AM1 semiempirical quantum-mechanics. As shown in Fig. 5, the MO electron density of the unprotonated form of FO$_x$P in the ground state is distributed symmetrically through the molecules. When the molecule is protonated, however, the situation of the orbital density distribution is quite different from an unprotonated form. The localization of the MO electron density, originated from the charge separation, is investigated in protonated forms that are strikingly different from each other according to the protonation position in an oxadiazole ring. As shown in Fig. 5, protonation at the nitrogen atom of N^1 makes the MO electron density in a fluorene unit deficient and, in contrast, that in a dimethoxyphenylene unit proficient. However, the protonation at the nitrogen atom of N^2 yields the opposite result. Judged by both ^{1}H NMR spectra of PFO$_x$EH and AM1 simulation mentioned above, the protonation probably occurs at the nitrogen atom in an oxadiazole ring close to a fluorene group due to the steric hindrance.

4. Conclusions

In conclusion, novel fully conjugated polyoxadiazoles having a fluorene group in the main chain, PFO$_x$ and PFO$_x$EH, were successfully prepared by the one-step and the two-step method, respectively. They have relatively high molecular weight and fairly good solubility to several common organic solvents. They show optically transductional properties as an acid receptor to a strong acid due to the very weak basicity of an oxadiazole ring, which can extend their applicability as a sensory material.

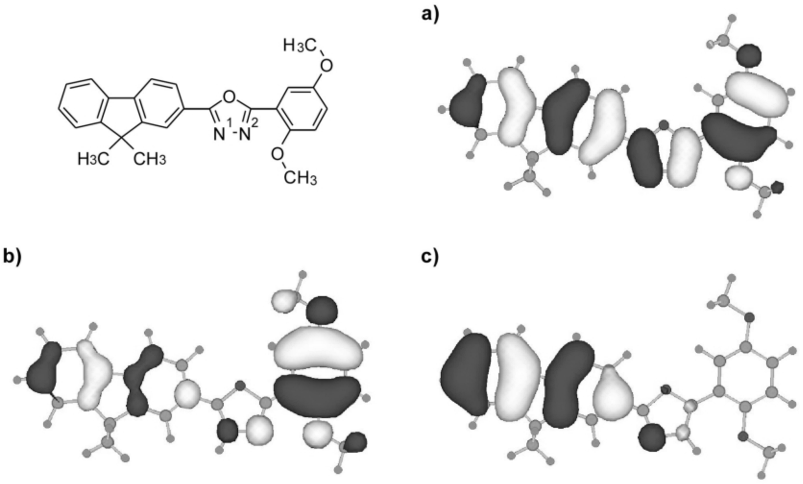

Fig. 5. The chemical structure of FO$_x$P and its isosurfaces of the OS in the ground state of (a) the unprotonated form, (b) the N^1-protonated form and (c) the N^2-protonated form. The orbital contour value is adjusted to 0.02.

References

[1] Swager TM. Acc Chem Res 1998;31:201.

[2] MacQuade DT, Pullen AE, Swager TM. Chem Rev 2000;100:2537.

[3] Fu DK, Xu B, Swager TM. Tetrahedron 1997;53:15487.

[4] Ng SC, Lu HF, Chan HSO, Fujii A, Laga T, Yoshino K. Macromolecules 2001;34:6895.

[5] Shetty AS, Liu EB, Lachicotte RJ, Jenekhe SA. Chem Mater 1999;11:2292.

[6] Jenekhe SA, Lu L, Alam MM. Macromolecules 2001;34:7315.

[7] Osaheni JA, Jenekhe SA. Macromolecules 1993;26:4726.

[8] So YH, Zaleski JM, Murlick C, Ellaboudy A. Macromolecules 1996;29:2783.

[9] Osaheni JA, Jenekhe SA. Macromolecules 1995;28:1172.

[10] Yamamoto T, Sugiyama K, Kanbara T, Hayashi H, Etori H. Macromol Chem Phys 1998;199:1807.

[11] Schulz B, Brehmer L. In: Salamone JC, editor. Polymeric Materials Encyclopedia, vol. 8. USA: CRC; 1996. p. 5595.

[12] Jenekhe SA, Johnson PO, Agrawal AK. Macromolecules 1989;22:3216.

[13] Schulz B. Mol Cryst Liq Cryst 1994;240:135.

[14] Yang NC, Choi HW, Suh DH. Polym Mater Sci Engng 2002;86:255.

[15] Eaton DF. Pure Appl Chem 1988;60:1107.

[16] Schulz B, Bruma M, Brehmer L. Adv Mater 1997;9:601.

[17] Maglio G, Palumbo R, Tortora M, Trifuoggi M, Varricchio G. Polymer 1998;39:6407.

[18] Huang W, Meng H, Yu WL, Gao J, Heeger AJ. Adv Mater 1998;10:593.

[19] Yu WL, Meng H, Pei J, Huang W. J Am Chem Soc 1998;120:11808.

[20] Trifonov RE, Ritshchev NI, Ostrovskii VA. Spectrochim Acta A 1996;52:1875.

[21] Zhang QT, Tour JM. J Am Chem Soc 1997;119:9624.

[22] Yao Y, Zhang QT, Tour JM. Macromolecules 1998;31:8600.

[23] Valeur B. Molecular Fluorescence: Principles and Applications. Weinheim: Wiley-VCH; 2002. Chapter 4.

[24] Eichen Y, Nakhmanovich G, Gorlik V, Epshtein O, Poplawski JM, Ehrenfreund E. J Am Chem Soc 1998;120:10463.

[25] Scheiner S, Kar T. J Phys Chem B 2002;106:534.